Robotica (2017) volume 35, pp. 1712–1731. © Cambridge University Press 2016
doi:10.1017/S026357471600045X

Bifurcations and symmetry in two optimal formation control problems for mobile robotic systems

Baoyang Deng, Michael O'Connor and Bill Goodwine*

Department of Aerospace & Mechanical Engineering, University of Notre Dame, Notre Dame, IN 46556 USA

(Accepted June 11, 2016. First published online: July 14, 2016)

SUMMARY

This paper studies bifurcations in the solution structure of an optimal control problem for mobile robotic formation control. In particular, this paper studies a group of mobile robots operating in a two-dimensional environment. Each robot has a predefined initial state and final state and we compute an optimal path between the two states for every robot. The path is optimized with respect to two factors, the control effort and the deviation from a desired "formation," and a bifurcation parameter gives the relative weight given to each factor. Using an asymptotic analysis, we show that for small values of the bifurcation parameter (corresponding to heavily weighting the control effort) a single unique solution is expected, and that as the bifurcation parameter becomes large (corresponding to heavily weighting maintaining the formation) a large number of solutions is expected. Between the asymptotic extremes, a numerical investigation indicates a solution bifurcation structure with a cascade of increasing numbers of solutions, reminiscent, but not the same as, period-doubling bifurcations leading to chaos in dynamical systems. Furthermore, we show that if the system is symmetric, the bifurcation structure possesses symmetries, and also present a symmetry-breaking example of a non-holonomic system. Knowledge and understanding of the existence and structure of bifurcations in the solutions of this type of formation control problem are important for robotics engineers because common optimization approaches based on gradient-descent are only likely to converge to the single nearest solution, and a more global study provides a deeper and more comprehensive understanding of the nature of this important problem in robotics.

KEYWORDS: Control of Robotic Systems; Mobile Robots; Motion Planning; Multi-Robot Systems; Path Planning; Robot Dynamics.

1. Introduction

Distributed and decentralized control has been an important area of research in recent years with a vast spectrum of applications ranging from, for example, robotic underwater vehicles,[1] satellite clustering,[2] electric power systems[3] to search and rescue operations.[4] An important subset of these problems is formation control for a system with multiple mobile robots. The approaches to the multi-robotic formation control problem are varied, but can be basically categorized into three groups: leader-follower methods,[5–7] behavior-based methods,[8–10] and virtual structure methods.[11–13] An excellent survey providing a comprehensive overview is by Murray.[14]

In this paper, the problem addressed is to determine the optimal trajectory for a formation of robots moving between specified initial and final configurations. The solution is optimized with respect to a combination of the control effort and the deviation from a desired formation. Therefore, the context of the problem we are considering would generally be offline path planning for the system prior to it executing its motion. Using standard methods from optimization, since each robot has its own predefined initial state and final state, the procedure to find the optimal path is to solve a two-point boundary value problem for a set of second-order ordinary differential equations. Obviously, not all

* Corresponding author. E-mail: bill@controls.ame.nd.edu
E-mails: moconn10@alumni.nd.edu, deng_baoyang@cat.com

https://doi.org/10.1017/S026357471600045X Published online by Cambridge University Press

formation control problems are best solved in this manner, but it is important because optimality is clearly a desired objective in the performance of any engineering system, including the area of formation control in mobile robotics.

The motivation for this work is to demonstrate some of the fundamental mathematical structure present in solutions to problems of this type. For many practical robotics problems, optimization methods are often a basic tool used. Because non-linear optimization methods can only guarantee a local optimum, a more global investigation of the relationship among the various extrema is informative. In this case, we isolate the relationship among the solutions to a single parameter which is natural in the problem and facilitates a systematic investigation. Some of the development of this work has been presented in a series of conference papers which developed the numerical bifurcation analysis,[15] a numerical homotopy solution method,[16] symmetry-breaking non-holonomic results[17] and some generalizations of the asymptotic analyses.[18]

As indicated, this paper particularly focuses on the relationship among multiple solutions for such systems. The existence of multiple non-trivial solutions of boundary value problems for non-linear second-order ordinary differential equations has been investigated by others. For example, for

$$\ddot{x} + a(t)f(x) = 0, \quad x(0) = 0, \quad x(1) = 0,$$

the properties of the solutions depend on the limiting behavior of the function $f(u)$. Erbe and Wang[19] studied the existence of *positive* solutions of the equation with linear boundary conditions. Specifically, for

$$f_0 = \lim_{s \to +0} \frac{f(s)}{s}, \quad f_\infty = \lim_{s \to +\infty} \frac{f(s)}{s},$$

they showed the existence of at least one positive solution in two cases: *superlinearity* ($f_0 = 0$, $f_\infty = \infty$) or *sublinearity* ($f_0 = \infty$, $f_\infty = 0$). Erbe, Hu and Wang[20] showed that there were at least two positive solutions in the case of superlinearity at one end (zero or infinity) and sublinearity at the other end. Naito and Tanaka[21] and Ma and Thompson[22] determined conditions based on the ratio $f(s)/s$ for the existence (or non-existence) of solutions. Their main result indicates that at least k solutions exist if the ratio $f(s)/s$ crosses the k eigenvalues of the associated eigenvalue problem. In other related work, Marcos do Ó, Lorca and Ubilla[23] use the fixed-point theorem of cone expansion/compression type, the upper–lower solutions method and degree arguments to study the existence, non-existence and multiplicity of positive solutions of the boundary value problem. Unfortunately, this prior work does not apply to the problem in this paper because of the structure of the equations and the relatively high dimensionality of robotic formation control problems, and hence the more fundamental investigation in this paper is needed.

There are other papers along similar lines.[24–40] Again unfortunately, none of these can be used for the problem at hand. All these papers are limited in one of the following three ways: consideration of positive solutions only, scalar equations or particular forms of non-linearity such as sub- or super-linearity. As will be shown subsequently, there is an interesting and rich structure to the nature of the relationship among solutions for our problem, which is indicative of the fact that a theory of bifurcations for boundary value problems of this type would be a useful mathematical development for engineers.

The organization of the rest of this paper is as follows. Section 2 presents the problem statement. Section 3 presents the solution bifurcation results and Section 4 presents the asymptotic analysis relating to the nature of the solutions for extreme cases. Section 5 presents the symmetry results and Section 6 presents a non-symmetric example wherein the symmetry is broken. Finally, Section 7 presents conclusions and outlines areas of potential future work.

2. Problem Statement

We first consider a standard fully-actuated system of the form

$$\dot{x} = u_1, \quad \dot{y} = u_2. \tag{1}$$

https://doi.org/10.1017/S026357471600045X Published online by Cambridge University Press

This is a canonical form for a fully actuated two-degree of freedom system. It may be considered as the equations of motion for a rolling sphere where the two inputs are the two angular velocities. While this is taken as a relatively simple starting point and we will refer to a collection of such systems in the rest of this section as a "fleet" of robots, these also can represent more complicated problems such as the kinematic equations governing spherical fingertips rolling on a flat surface,[41] in which case the formation control problem we consider is related to optimal grasping and dexterous manipulation in robotics.

We consider a fleet of n of such robots with states $(x_i, y_i), i \in \{1, \ldots, n\}$. The problem is to find the control inputs $u_{i_1}(t), u_{i_2}(t)$ for each robot i, which steer a formation of robots of this type from a start configuration to a goal configuration, while maintaining, to some degree, the formation throughout the execution of the motion. This is achieved by minimizing the functional

$$J = \int_0^{t_f} \sum_{i=1}^{n} \left(\left(u_{i_1}\right)^2 + \left(u_{i_2}\right)^2 \right) + \sum_{i=1}^{n-1} k \left(d_i - \overline{d}\right)^2 dt,$$

subject to the robotic kinematic constraints in Eq. (1), where $n > 2$ is the number of robots, $d_i = \sqrt{(x_i - x_{i+1})^2 + (y_i - y_{i+1})^2}$ is the distance between the ith and $(i+1)$th robots, $\overline{d}$ is the desired distance between two adjacent robots, and k is a weighting factor (ultimately to become a bifurcation parameter). The first term in the sum in the functional is the control effort and the second is a penalty for deviations from the desired formation, which in this case is simply attempting to maintain a desired distance between neighboring robots. If the weighting constant k is small, then minimizing the control effort is more important than maintaining the formation, and conversely if k is large, maintaining the formation is more important than minimizing the control effort.

We note that because the cost functional includes control effort terms, which depend on the specific robots' kinematics or dynamics, different types of robots will have different solutions to this problem. This particular type of formation, maintaining distance, is important in robotics because control of formations of networked robots is only enabled by effective communication,[42] which can be maintained by ensuring line-of-site and range constraints. Furthermore, it is relatively simple so that our analysis can be more transparently focused on the trade-off between control effort and maintaining distance between the robots.

Either Pontryagin's maximum principle or calculus of variations may be used to determine the differential equations which have solutions which are extrema of the cost functional. Specifically, this results in

$$u_{i_1} = \frac{1}{2} p_{i_1}, \quad u_{i_2} = \frac{1}{2} p_{i_2},$$

and equations of motion

$$\begin{aligned}
\dot{x}_i &= \frac{1}{2} p_{i_1} \\
\dot{y}_i &= \frac{1}{2} p_{i_2} \\
\dot{p}_{i_1} &= \frac{2k\,(x_i - x_{i-1})\left(d_{i-1} - \overline{d}\right)}{d_{i-1}} + \frac{2k\,(x_i - x_{i+1})\left(d_i - \overline{d}\right)}{d_i} \\
\dot{p}_{i_2} &= \frac{2k\,(y_i - y_{i-1})\left(d_{i-1} - \overline{d}\right)}{d_{i-1}} + \frac{2k\,(y_i - y_{i+1})\left(d_i - \overline{d}\right)}{d_i}.
\end{aligned} \tag{2}$$

Because they correspond to the robots at the two ends of the formation, the last two equations in Eq. (2) only have the second term in the sum when $i = 1$ and they only have the first term in the sum when $i = n$. This is because there is no 0 robot or $n + 1$ robot, but we do not write a separate set of equations for the end robots for simplicity.

https://doi.org/10.1017/S026357471600045X Published online by Cambridge University Press

In this paper, the following specific boundary conditions are considered:

$$\begin{aligned} x_i(0) &= c + (i-1)\overline{d}, \\ x_i(1) &= 0, \\ y_i(0) &= 0, \\ y_i(1) &= c + (i-1)\overline{d}, \end{aligned} \tag{3}$$

where c is a constant. These correspond to an initial formation with the robots arranged along the x-axis starting with the first robot at $x = c$ with a distance $\overline{d}$ between each robot and a final formation with the robots arranged along the y-axis starting with the first robot at $y = c$ with a distance of $\overline{d}$ between each robot. Because the initial and final formations are not parallel, straight-line trajectories satisfying the boundary conditions will not maintain the desired distance between the robots. Thus, a solution that minimizes the control effort, which will be a straight line, will not maintain the desired formation, and the relative weighting of the two terms in the cost function will be important and affect the solution.

We emphasize that this paper focuses on the nature of the solutions to this optimization problem, determined from the two-point boundary value problems given in Eqs. (2) and (3). In interacting robotic systems, a solution which must balance the relative positions among the robots with other considerations such as path length is of great practical importance, and the focus of this paper is on the theoretical development and complexities associated with such considerations. As will be shown subsequently, the nature of the solution structure to these equations is complicated and can be characterized by bifurcation diagrams. Any real implementation of these results will have to address the significant challenges posed by wheel slippage, encoder resolution, sensor accuracy, etc. However, the qualitative nature of the solutions obtained is such that they would be neither more nor less difficult to track than solutions obtained by other trajectory generation methods.

3. Bifurcation Results

This section presents bifurcation diagrams which were obtained from numerical simulations. The next sections present an analysis which predicts certain aspects of the structure of these bifurcation diagrams. For a system containing n robots, when the weighting constant k is given, an optimal trajectory can be obtained numerically by solving the equations of motion given by Eq. (2) using various methods such as the shooting method[43] or a finite-difference method.[44] In this paper, we used both methods (the numerical results in this section were obtained using the shooting method and the results in Section 6 were obtained using the finite-difference method) and verified convergence of the methods to ensure accuracy of the solutions. In this section, we will present simulations for a five-robot system and seven-robot system.

This paper considers how the solutions for the system bifurcate as the parameter k varies. It is emphasized that such bifurcations have important distinctions from standard bifurcations from dynamical systems theory which considers bifurcations of *fixed points* of a dynamical system. For the systems considered in this paper, we are considering solutions to *boundary value problems*, in contrast to initial value problems. Of course, solutions to the boundary value problem are fixed points of variations of the cost function; however, the entire solution is the fixed point and we want to quantify the bifurcations in a physically meaningful way. Hence, it is necessary from the beginning to define the manner in which we are quantifying the bifurcations.

To start, consider the solutions for a seven-robot system illustrated in Fig. 1. The robots are initially arranged evenly spaced along the horizontal axis, and the final configuration is for them to be evenly spaced along the vertical axis. In the case illustrated $k = 23$, $c = 4$ and $\overline{d} = 2$ and a total of 10 different solutions satisfying both the differential equations and boundary conditions were found. The right figure in Fig. 1 illustrates the trajectories for the fifth robot with the deviation from the nominal trajectory magnified to more clearly illustrate the relationship among the solutions. The goal of the rest of this section is to start to investigate the relationship among these multiple solutions and how they come about. To do this, we first consider a simpler five-robot system, and then return to this seven-robot system.

https://doi.org/10.1017/S026357471600045X Published online by Cambridge University Press

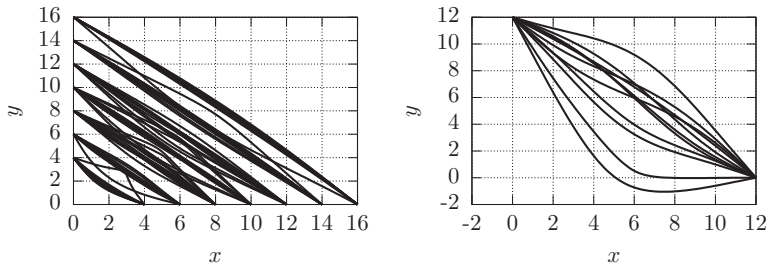


Fig. 1. Optimal paths for a seven robot system with $k = 23$.

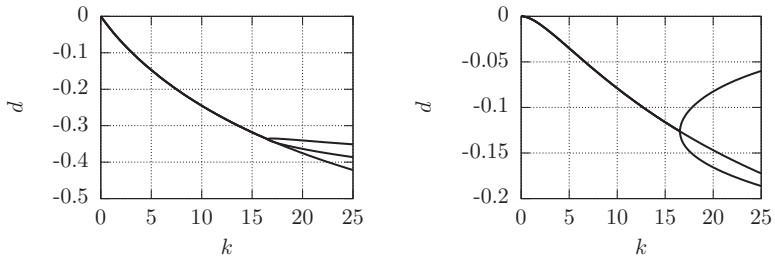


Fig. 2. Bifurcation diagrams for a five robot system: robot one (left) and robot two (right).

3.1. Bifurcations of solutions for a five-robot system

Because k is a parameter in differential equations, it will clearly affect the solutions. In fact, as k is varied, the nature and number of solutions changes. In order to present the relationship between the number of solutions and k, we construct bifurcation diagrams. Because a straight line connecting the end points is the optimal solution when $k = 0$, we will designate that as a *nominal trajectory* and the measure of the difference between solutions we use is the signed distance from the solution to the straight line nominal solution at some specified time. Solutions above the nominal trajectory have a positive distance and those below a negative distance. As long as different solutions are not intersecting at that time, this would provide a measure of difference between different solutions. For the rest of this paper in all the bifurcation diagrams, $t = 0.25$ is used as the time to measure the differences between solutions (recall $t \in [0, 1]$).

Remark. What measure best represents the difference between solutions in a boundary value problem is not a straight-forward question. Recall that in standard dynamical systems theory, bifurcation diagrams usually represent the value and stability of fixed points or equilibria of a dynamical system. While an entire solution in the boundary value problems, we consider is a type of fixed point of a variational problem, differences along the entire trajectory may be important. Some sort of norm is appealing; however, solutions that in a sense are "opposite" such as the solutions crossing each other near the point (6, 6) on the right in Fig. 1 would be hard to distinguish due to the fact a norm is positive semi-definite. The results in this paper are adequately communicated using a simple "difference at $t = 0.25$" measure and we leave as an open research question what the best measure would be for specific problems or specific applications.

The plots in Figs. 2–4 illustrate this measure of the difference between solutions for each robot in the five robot system as k is varied from 0 to 25. In these bifurcation diagrams, the first robot is the one with the shortest trajectory, the fifth robot is the one with the longest trajectory and they are ordered sequentially. Observe that the bifurcation diagrams for robots 1 and 5 are symmetric reflections to each other about the $d = 0$ axis and the bifurcation diagrams for robots two and four are similarly symmetric (even though each follows a trajectory with a different length). Finally, the bifurcation diagram for robot three is symmetric to itself about $d = 0$ axis. We will prove this feature *must* be present in this system subsequently in Section 5.

https://doi.org/10.1017/S026357471600045X Published online by Cambridge University Press

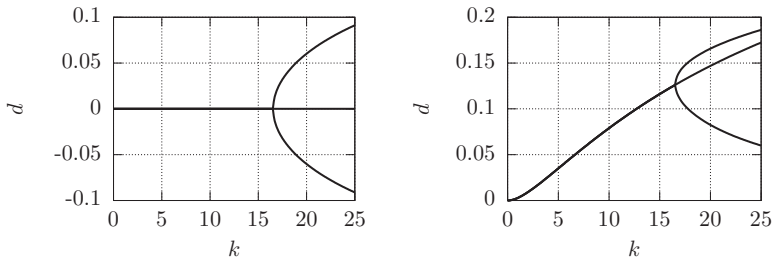


Fig. 3. Bifurcation diagrams for a five robot system: robot three (left) and robot four (right).

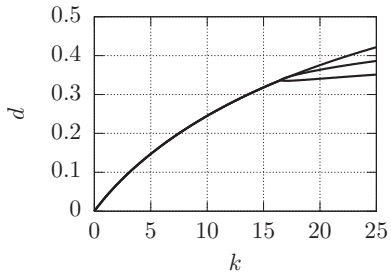


Fig. 4. Bifurcation diagrams for a five robot system: robot five.

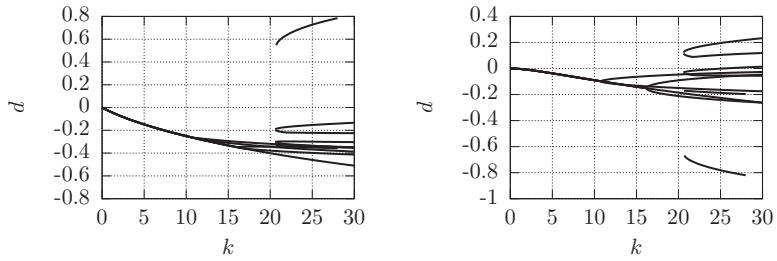


Fig. 5. Bifurcation diagrams for a seven robot system:robot one (left) and robot two (right).

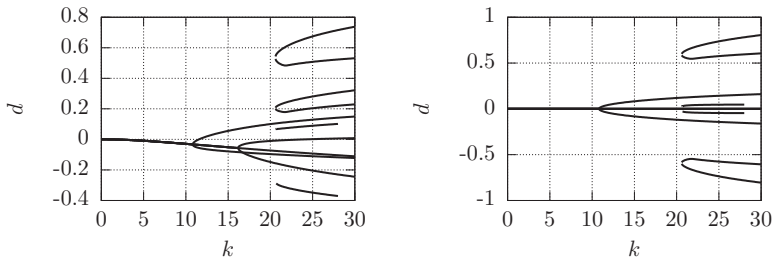


Fig. 6. Bifurcation diagrams for a seven robot system: robot three (left) and robot four (right).

3.2. Bifurcations of solutions for a seven robot system

Figures 5–8 illustrate the bifurcation diagrams for the solutions versus k constructed in a manner identical to that of the system of five robots. Observe that, similar to the five robot case, the bifurcation diagrams for robots one and seven are symmetric to each other about $d = 0$ axis as are the bifurcation diagrams for robots two and six and robots three and five, and the bifurcation diagram for robot 4 is symmetric to itself about $d = 0$ axis.

In the seven-robot bifurcation diagrams, some of the solution branches do not have upper and lower branches, i.e., they are neither diffeomorphic to a pitchfork nor "sideways parabolas." Instead, there is a single branch with an isolated starting point. One appears near the top of the bifurcation diagram on the right for robot one in Fig. 5, for example. One would expect a second connected branch to that, but extensive numerical searching did not find one. Perhaps the branch is unstable

https://doi.org/10.1017/S026357471600045X Published online by Cambridge University Press

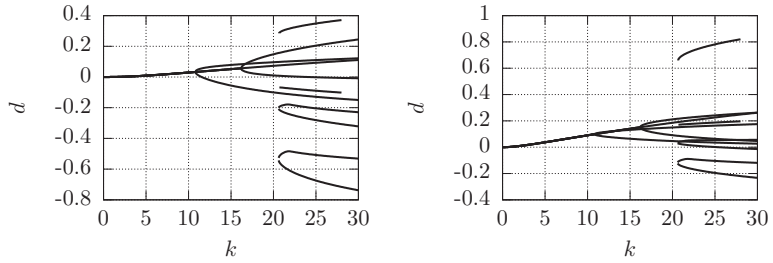


Fig. 7. Bifurcation diagrams for a seven robot system: robot five (left) and robot six (right).

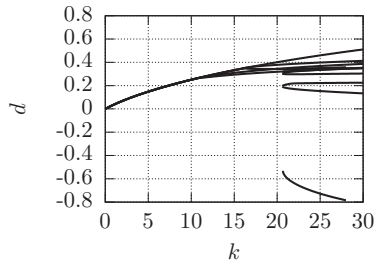


Fig. 8. Bifurcation diagrams for a seven robot system: robot seven.

in a sense that a numerical method will not converge to it, or perhaps there is not a second branch. Regardless, the nature of the single branch solutions on the bifurcation diagrams is an open research question.

Subsequently, we show that the bifurcation diagrams must be symmetric. Given the current state of the art, this is useful because we are limited to a numerical search for solutions. Having found one solution, it would be nice to automatically have another solution associated with it. From a very practical perspective, one aspect of this problem is that global non-linear optimization problems may (usually!) have multiple local extrema, and searching for them in order to find the best of the ones that were found can be expensive. Also, a close inspection reveals that while the bifurcation diagrams are symmetric, the solutions themselves are not. Hence, we cannot simply "flip" some solutions around.

In both the five-robot and seven-robot systems, the bifurcation diagrams indicated one solution for small values of k with bifurcations leading to an increasing number of solutions for increasing k. This structure makes sense. When k is zero, there is no coupling among the robots and the trajectory minimizing the control effort is a straight line connecting the boundary conditions. In the limit as $k \to \infty$, maintaining the formation is more important than the control effort. In the limit, *any* trajectory that maintains the formation regardless of the length of the trajectory will be a solution. Hence, the structure exhibited in the bifurcation diagrams has an appealing intuitive basis. The analysis in the next section shows this interpretation conforms to the mathematical structure of the problem.

4. Asymptotic Analysis

Because the governing equations are non-linear, global results are, of course, difficult to obtain. The bifurcation diagrams, we present were all obtained via exhaustive numerical searches. Such a method, however, clearly does not preclude the existence of solutions we did not find. This section validates the *qualitative* dependence of the number of solutions on the bifurcation parameter. In the cases of very small k and very large k, we may use an asymptotic expansion to investigate the effect of k on the number of solutions to the optimization problem. As will be shown, this analysis is consistent with the existence of a unique solution for small values of k and many solutions for very large values of k, which is the pattern indicated in the numerical results.

https://doi.org/10.1017/S026357471600045X Published online by Cambridge University Press

4.1. Small k

We use a standard perturbation method[45,46] to determine a series expansion for solutions to Eq. (2) for $k \ll 1$. If we let

$$\begin{aligned}
x_i &= x_{i,0} + kx_{i,1} + k^2 x_{i,2} + k^3 x_{i,3} + \cdots + k^j x_{i,j} + \cdots, \\
y_i &= y_{i,0} + ky_{i,1} + k^2 y_{i,2} + k^3 y_{i,3} + \cdots + k^j y_{i,j} + \cdots, \\
p_{i_1} &= p_{i_1,0} + kp_{i_1,1} + k^2 p_{i_1,2} + k^3 p_{i_1,3} + \cdots + k_j p_{i_1,j} + \cdots, \\
p_{i_2} &= p_{i_2,0} + kp_{i_2,1} + k^2 p_{i_2,2} + k^3 p_{i_2,3} + \cdots + k_j p_{i_2,j} + \cdots,
\end{aligned}$$

and substitute into the equations of motion (Eq. (2)), a set of *linear* differential equations is obtained for each power of the expansion parameter k. A reader interested in further details on the nature and structure of the asymptotic expansion for all orders of this system is referred to Deng.[47]

Specifically, the leading-order equation corresponding to k^0 terms gives the set of *linear* equations for the ith robot of the form

$$\dot{x}_{i,0} = \frac{1}{2} p_{i_1,0}, \quad \dot{y}_{i,0} = \frac{1}{2} p_{i_2,0}, \quad \dot{p}_{i_1,0} = 0, \quad \dot{p}_{i_2,0} = 0,$$

with boundary conditions

$$x_{i,0}(0) = x_{1,0}(0) + (i-1)\overline{d}, \quad y_{i,0}(0) = 0, \quad x_{i,0}(1) = 0, \quad y_{i,0}(1) = y_{1,0}(1) + (i-1)\overline{d}.$$

These are easy to solve by direct integration and have solutions of the form

$$x_{i,0} = -x_{i,0}(0)t + x_{i,0}(0), \quad y_{i,0} = y_{i,0}(1)t, \quad p_{i_1,0} = -2x_{i,0}(0), \quad p_{i_2,0} = 2y_{i,0}(1).$$

Naturally, these are straight line, constant velocity solutions, which is expected when the only component of the cost function is the control effort and the zeroth-order solution does not contain k.

The k^1th order equations are of the form

$$\begin{aligned}
\dot{x}_{i,1} &= \frac{p_{i_1,1}}{2} \\
\dot{y}_{i,1} &= \frac{p_{i_2,1}}{2} \\
\dot{p}_{i_1,1} &= 2\left(\frac{(x_{i,0} - x_{i-1,0})(d_{i-1,0} - \overline{d})}{d_{i-1,0}} + \frac{(x_{i,0} - x_{i+1,0})(d_{i,0} - \overline{d})}{d_{i,0}} \right) \\
\dot{p}_{i_2,1} &= 2\left(\frac{(y_{i,0} - y_{i-1,0})(d_{i-1,0} - \overline{d})}{d_{i-1,0}} + \frac{(y_{i,0} - y_{i+1,0})(d_{i,0} - \overline{d})}{d_{i,0}} \right),
\end{aligned} \tag{4}$$

where $d_{i,0}$ is the distance term as a function of the zeroth-order solutions. Because the boundary conditions do not depend on k, only the zeroth-order equations have non-zero boundary conditions. That is, the zeroth-order equations have the actual boundary conditions and all the higher-order equations have homogeneous boundary conditions.

The equations corresponding to higher orders of k are obtained similarly, but naturally grow in complexity. Observe, as is the usual case for an asymptotic analysis, that the differential equations for k^1 depend only on $x_{i,1}$, $y_{i,1}$, $p_{i_1,1}$ and $p_{i_2,1}$ and the *lower order solutions*. Hence, the solutions for the zeroth-order equations appear as inhomogenous terms in the first-order equations, and so on recursively.

Because the first-order costate equations only depend on the lower-order solutions they may be solved by direct integration. Once the first-order costates are determined, $x_{i,1}$ and $y_{i,1}$ may be obtained by direct integration. There will be four constants of integration which may be used to satisfy the four boundary conditions. Also, because the zeroth-order solutions are continuous and bounded, a

https://doi.org/10.1017/S026357471600045X Published online by Cambridge University Press

unique solution for each integral exits. This is consistent with the solution in the neighborhood of the straight-line $k = 0$ zeroth-order solution being unique, which is furthermore consistent with the physical interpretation that when the formation weighting is zero, the only optimal solution is the one that minimizes the path length, i.e., a straight line.

Because the zeroth-order solutions are straight lines, only the first and nth equations will have non-zero solutions for the first-order equations. This is due to the fact that straight lines are of the nature that the $(i-1)$th and $(i+1)$th robots' effect on the ith robot cancel. This is evident from Eq. (4) because the right-hand side of the costate equations depend only on the zeroth-order solutions, and hence the difference in the distances will be the same and the difference in the x or y components of the two neighbors will be the same magnitude with opposite sign. Hence, the costate equations will have constant solutions. Therefore, because the end robots do not have a neighbor on each side, they are the only robots that will have a first-order effect from k. Space limitations prevent including the higher-order equations, but the second from the end robots have a zero first-order solution, but non-zero second-order solution, and so on. Hence, the deviation from the straight-line solution is of increasingly higher order in k toward the middle of the formation. This is consistent with an intuitive idea that robots near the outside of the formation have greater flexibility in their path to move away from the straight line; whereas, robots in the middle are "squeezed" by the formation.

4.2. Large k

Now, we consider the other extreme, a very large formation weighting parameter. For large k ($1/k \ll 1$), a similar asymptotic expansion is used to solve Eq. (2) but instead of k, $\epsilon = 1/k$ is used as the expansion parameter. Similar to before, let

$$\begin{aligned}
x_i &= x_{i,0} + \epsilon x_{i,1} + \epsilon^2 x_{i,2} + \epsilon^3 x_{i,3} + \cdots + \epsilon^j x_{i,j} + \cdots, \\
y_i &= y_{i,0} + \epsilon y_{i,1} + \epsilon^2 y_{i,2} + \epsilon^3 y_{i,3} + \cdots + \epsilon^j y_{i,j} + \cdots, \\
p_{i_1} &= p_{i_1,0} + \epsilon p_{i_1,1} + \epsilon^2 p_{i_1,2} + \epsilon^3 p_{i_1,3} + \cdots + \epsilon_j p_{i_1,j} + \cdots, \\
p_{i_2} &= p_{i_2,0} + \epsilon p_{i_2,1} + \epsilon^2 p_{i_2,2} + \epsilon^3 p_{i_2,3} + \cdots + \epsilon_j p_{i_2,j} + \cdots.
\end{aligned}$$

We obtain the following equation for leading order of ϵ:

$$\begin{aligned}
\dot{x}_{i,0} &= \frac{1}{2} p_{i_1,0} \\
\dot{y}_{i,0} &= \frac{1}{2} p_{i_2,0} \\
0 &= \frac{2k\left(x_{i,0} - x_{i-1,0}\right)\left(d_{i-1,0} - \overline{d}\right)}{d_{i-1,0}} + \frac{2k\left(x_{i,0} - x_{i+1,0}\right)\left(d_{i,0} - \overline{d}\right)}{d_{i,0}} \\
0 &= \frac{2k\left(y_{i,0} - y_{i-1,0}\right)\left(d_{i-1,0} - \overline{d}\right)}{d_{i-1,0}} + \frac{2k\left(y_{i,0} - y_{i+1,0}\right)\left(d_{i,0} - \overline{d}\right)}{d_{i0}}.
\end{aligned}$$

The last two equations may be simplified to

$$(x_{i,0} - x_{i-1,0})^2 + (y_{i,0} - y_{i-1,0})^2 = \overline{d}^2, \tag{5}$$

which transparently shows that the limit for large k requires that the distance constraint be exactly maintained.

Since the third and fourth equations are algebraic (as is Eq. (5)), then the costates, p are unconstrained and hence *any* path that maintains the desired distance between the robots and satisfies the boundary conditions is a solution to these equations. This makes physical sense because in the limit as $k \to \infty$, the control effort becomes negligible relative to the formation constraint. Hence, in the limit of very large k, the asymptotic analysis indicates that there is an infinite number of solutions. As long as the separation distance is maintained and the boundary conditions are satisfied, any path is optimal.

https://doi.org/10.1017/S026357471600045X Published online by Cambridge University Press

4.3. Generalization of asymptotic results

Up to this point, the results in this section are for the specific example in this paper. Now, we consider a more general class of systems to which similar results will apply. To do this, we consider a more general cost functional, which will naturally lead to a more general class of differential equations governing the dynamics of the system. It is natural and commonplace to minimize the control effort, so we generalize the formation function component of the functional. Specifically, let

$$J = \int_0^{t_f} \sum_{i=1}^{n} \left(\left(u_{i_1}\right)^2 + \left(u_{i_2}\right)^2 \right) + \sum_{i=1}^{n-1} kf(x_1, x_2, \ldots, x_n, y_1, y_2, \ldots, y_n)dt,$$

where the function, f, is a differentiable function of the relative configuration of the robots that is minimized when the robots are in the desired formation. Calculus of variations yields

$$\dot{x}_i = \frac{1}{2}p_{i_1}, \quad \dot{y}_i = \frac{1}{2}p_{i_2}, \quad \dot{p}_{i_1} = 2k\frac{\partial f}{\partial x_i}, \quad \dot{p}_{i_2} = 2k\frac{\partial f}{\partial y_i}.$$

Following the same asymptotic analysis as above, it is clear that for $k \ll 1$, we have

$$\dot{x}_i = \frac{1}{2}p_{i_1}, \quad \dot{y}_i = \frac{1}{2}p_{i_2}, \quad \dot{p}_{i_1} = 0, \quad \dot{p}_{i_2} = 0,$$

again, yielding straight-line solutions, and when $k \gg 1$, we have

$$\dot{x}_i = \frac{1}{2}p_{i_1}, \quad \dot{y}_i = \frac{1}{2}p_{i_2}, \quad 0 = 2k\frac{\partial f}{\partial x_i}, \quad 0 = 2k\frac{\partial f}{\partial y_i},$$

which is satisfied by *any* trajectory when the formation function is minimized. Hence, as was the case for the very specific system we considered, the same results hold for *any* formation function which is differentiable and minimized when the formation is satisfied. Specifically, there is a unique solution for small k and infinitely many solutions in the limit as $k \to \infty$, suggesting a cascade of bifurcations qualitatively the same as we found for the specific system considered in this paper.

5. Symmetries in the Bifurcation Diagrams

This section proves that the symmetries found in the numerically constructed bifurcation diagrams must be present. This is of practical value because it reduces the computation time necessary in a search over multiple solutions since a second solution can always be found from any solution that is obtained that is not symmetric with itself. This is related to some of our prior work focusing on model reduction for symmetric systems.[48–54]

Suppose $(x_1, x_2, \ldots, x_n, y_1, y_2, \ldots, y_n)$ is a solution of Eq. (2) with the boundary conditions in Eq. (3), and let

$$x_i = (x_s)_i + (x_d)_i, \quad y_i = (y_s)_i + (y_d)_i,$$

where

$$(x_s)_i = (c + (i-1)\bar{d})(1-t), \quad (y_s)_i = (c + (i-1)\bar{d})t.$$

The subscripts s indicate a "straight-line" solution and the subscripts d indicate the component of the solution that is a "deviation" from the straight line. If $v(t) = ((x_d)_1, (y_d)_1, \ldots, (x_d)_n, (y_d)_n)$, then $(x_d)_i, (y_d)_i, i = 1, 2, \ldots, n$, satisfy the following equations with homogeneous boundary conditions:

$$-(\ddot{x}_d)_i(t) = f_i(v(t)), \quad -(\ddot{y}_d)_i(t) = g_i(v(t)), \tag{6}$$

where $f_1 = h_1$, $g_1 = l_1$, $f_n = -h_{n-1}$, $g_n = -l_{n-1}$, and for $i = (2, 3, \ldots, n-1)$

$$f_i = h_i - h_{i-1}, \quad g_i = l_i - l_{i-1},$$

https://doi.org/10.1017/S026357471600045X Published online by Cambridge University Press

where, for all $i = (1, 2, \ldots, n)$

$$h_i = \left(\frac{\overline{d}}{d_i} - 1\right)\left(-\overline{d} + \overline{d}t + (x_d)_i - (x_d)_{i+1}\right),$$

$$l_i = \left(\frac{\overline{d}}{d_i} - 1\right)\left(-\overline{d}t + (y_d)_i - (y_d)_{i+1}\right),$$

$$d_i = \sqrt{\left(-\overline{d} + \overline{d}t + (x_d)_i - (x_d)_{i+1}\right)^2 + \left(-\overline{d}t + (y_d)_i - (y_d)_{i+1}\right)^2}.$$

The system in Eq. (6), is equivalent to the system of integral equations

$$(x_d)_i = \int_0^1 G(t, s) f_i(v(s))ds, \quad (y_d)_i = \int_0^1 G(t, s) g_i(v(s))ds, \tag{7}$$

where $G(t, s)$ is the Green's function of the differential operator $-\ddot{u} = 0$ with homogeneous boundary conditions, where $u = x_{d_i}$ or $u = y_{d_i}$, and

$$G(t, s) = \begin{cases} t(1 - s), & t \leq s \\ s(1 - t), & t > s \end{cases}.$$

If A_i, B_i and F are maps such that

$$A_i v(t) = k \int_0^1 G(t, s) f_i(v(s))ds,$$

$$B_i v(t) = k \int_0^1 G(t, s) g_i(v(s))ds,$$

$$Fv(t) = (A_1(v)(t), B_1(v)(t), \ldots, A_n(v)(t), B_n(v)(t)),$$

then determining a solution to Eq. (7) is equivalent to finding a fixed point to equation

$$Fv(t) = v(t). \tag{8}$$

The following proposition proves that if a solution is known, then the "opposite" deviation from the straight-line solution is also a solution for the robot on the other side of the formation.

Proposition 1. Suppose $v(t)$ is a fixed point of Eq. (8). Let

$$(\hat{x}_d)_{n+1-i} = -(x_d)_i, \quad (\hat{y}_d)_{n+1-i} = -(y_d)_i, \tag{9}$$

and $\hat{v}(t) = ((\hat{x}_d)_1, (\hat{y}_d)_1, \ldots, (\hat{x}_d)_n, (\hat{y}_d)_n)$, then $\hat{v}(t)$ is also a fixed point of Eq. (8).

Proof. Substituting for the definition of the hat terms for each gives:

$$\begin{aligned} d_i &= \sqrt{\left(-\overline{d} + \overline{d}t + (x_d)_i - (x_d)_{i+1}\right)^2 + \left(-\overline{d}t + (y_d)_i - (y_d)_{i+1}\right)^2} \\ &= \sqrt{\left(-\overline{d} + \overline{d}t - (\hat{x}_d)_{n+1-i} + (\hat{x}_d)_{n-i}\right)^2 + \left(-\overline{d}t - (\hat{y}_d)_{n+1-i} + (\hat{y}_d)_{n-i}\right)^2} \\ &= \sqrt{\left(-\overline{d} + \overline{d}t + (\hat{x}_d)_{n-i} - (\hat{x}_d)_{n-i+1}\right)^2 + \left(-\overline{d}t + (\hat{y}_d)_{n-i} - (\hat{y}_d)_{n-i+1}\right)^2} \\ &= \hat{d}_{n-i} \end{aligned}$$

https://doi.org/10.1017/S026357471600045X Published online by Cambridge University Press

$$
\begin{aligned}
h_i &= \left(\frac{\overline{d}}{d_i} - 1\right)\left(-\overline{d} + \overline{d}t + (x_d)_i - (x_d)_{i+1}\right) \\
&= \left(\frac{\overline{d}}{\hat{d}_{n-i}} - 1\right)\left(-\overline{d} + \overline{d}t - (\hat{x}_d)_{n+1-i} + (\hat{x}_d)_{n-i}\right) \\
&= \left(\frac{\overline{d}}{\hat{d}_{n-i}} - 1\right)\left(-\overline{d} + \overline{d}t + (\hat{x}_d)_{n-i} - (\hat{x}_d)_{n-i+1}\right) \\
&= \hat{h}_{n-i} \\
l_i &= \left(\frac{\overline{d}}{d_i} - 1\right)\left(-\overline{d}t + (y_d)_i - (y_d)_{i+1}\right) \\
&= \left(\frac{\overline{d}}{\hat{d}_{n-i}} - 1\right)\left(-\overline{d}t - (\hat{y}_d)_{n+1-i} + (\hat{y}_d)_{n-i}\right) \\
&= \left(\frac{\overline{d}}{\hat{d}_{n-i}} - 1\right)\left(-\overline{d}t + (\hat{y}_d)_{n-i} - (\hat{y}_d)_{n-i+1}\right) \\
&= \hat{l}_{n-i},
\end{aligned}
$$

and

$$
\begin{aligned}
f_1 &= h_1 = \hat{h}_{n-1} = -\hat{f}_n \\
g_1 &= l_1 = \hat{l}_{n-1} = -\hat{g}_n \\
f_i &= h_i - h_{i-1} = \hat{h}_{n-i} - \hat{h}_{n+1-i} = -\hat{f}_{n+1-i} \\
g_i &= l_i - l_{i-1} = \hat{l}_{n-i} - \hat{h}_{n+1-i} = -\hat{g}_{n+1-i} \\
f_n &= -h_{n-1} = -\hat{h}_1 = -\hat{f}_1 \\
g_n &= -l_{n-1} = -\hat{l}_1 = -\hat{g}_1,
\end{aligned}
$$

which gives

$$
f_i = -\hat{f}_{n+1-i}, \quad g_i = -\hat{g}_{n+1-i},
$$

for all i from 0 to n. Then,

$$
\begin{aligned}
(\hat{x}_d)_i &= -(x_d)_{n+1-i} = -\int_0^1 G(t,s) f_{n+1-i} ds = \int_0^1 G(t,s)\hat{f}_i ds \\
(\hat{y}_d)_i &= -(y_d)_{n+1-i} = -\int_0^1 G(t,s) g_{n+1-i} ds = \int_0^1 G(t,s)\hat{g}_i ds.
\end{aligned}
$$

Hence, $\hat{v}(t) = ((\hat{x}_d)_1, (\hat{y}_d)_1, \ldots, (\hat{x}_d)_n, (\hat{y}_d)_n)$ is a solution of Eq. (8). □

Equation (9) gives an algebraic expression for the symmetric solutions, which is useful because the theorem proves they satisfy the boundary value problems and hence reduces the computational burden of determining additional solutions via computationally intensive methods such as the shooting method or finite-difference method. Note that the relationship is not simply the opposite deviation from the straight line solution, but is the opposite deviation from the straight line for a *different* robot.

https://doi.org/10.1017/S026357471600045X Published online by Cambridge University Press

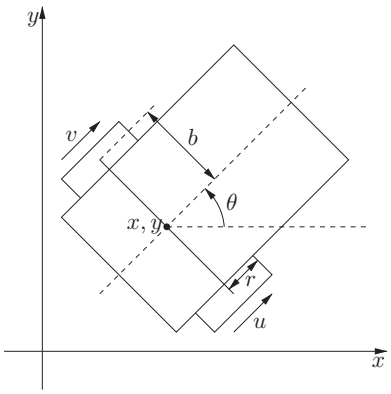


Fig. 9. Kinematic model.

6. Symmetry-Breaking Example

This section presents a mobile robot formation control problem that is superficially similar to the one already considered, but where the symmetry of the bifurcations is broken. While the boundary conditions for the problem are similarly "symmetric," it is the robot itself, perhaps surprisingly, that breaks the symmetry, illustrating that while the cascade of bifurcations may be a relatively common feature in formation control, the symmetric nature of the bifurcations is more limited. Furthermore, as indicated previously, while we verified convergence of all of our numerical solutions, we include this section because we use a different numerical approach than in the previous sections. Because the symmetry-breaking in this section is slight, it is important to ensure it is not an artifact of the numerical method.

The model considered is a standard two-wheeled non-holonomic mobile robot,[55] as is illustrated in Fig. 9. Kinematically, it resembles a wheelchair, having three degrees of freedom and two control inputs. Hence, it is underactuated by one degree of freedom. The state variables are x, y, and θ, which correspond to the three degrees of freedom and the control inputs are u and v, the angular velocities of the wheels. For all the simulations in this paper, we adopt more physically realistic, non-normalized parameter values. Specifically, the model parameters are taken to be $r = 0.02$ and $b = 0.05$ with overall trajectory lengths of $\mathcal{O}(1)$, corresponding to the robot traversing a trajectory that is large relative to its size.

Assuming a rolling without slipping condition for each wheel, the kinematics are described by three non-holonomic constraints

$$\dot{x} = \frac{r}{2}\cos\theta(u+v), \quad \dot{y} = \frac{r}{2}\sin\theta(u+v), \quad \dot{\theta} = \frac{r}{2b}(u-v).$$

Using a standard calculus of variations approach with the cost functional which minimizes the control effort

$$L^* = \frac{1}{2}(u^2+v^2) + \lambda_x\left(\dot{x} - \frac{r}{2}\cos\theta(u+v)\right) + \lambda_y\left(\dot{y} - \frac{r}{2}\sin\theta(u+v)\right) + \lambda_\theta\left(\dot{\theta} - \frac{r}{2b}(u-v)\right),$$

we obtain following ordinary differential equations for optimal solutions

$$\begin{aligned}
\dot{x} &= \frac{r}{2}\cos\theta(u+v), & \dot{\lambda}_x &= 0\\
\dot{y} &= \frac{r}{2}\sin\theta(u+v), & \dot{\lambda}_y &= 0\\
\dot{\theta} &= \frac{r}{2b}(u-v), & \dot{\lambda}_\theta &= \frac{r}{2}(u+v)(\lambda_x\sin\theta - \lambda_y\cos\theta),
\end{aligned}$$

https://doi.org/10.1017/S026357471600045X Published online by Cambridge University Press

where

$$u = \frac{r}{2}\left(\lambda_x \cos\theta + \lambda_y \sin\theta + \frac{1}{b}\lambda_\theta\right), \quad v = \frac{r}{2}\left(\lambda_x \cos\theta + \lambda_y \sin\theta - \frac{1}{b}\lambda_\theta\right).$$

For this system, we use a finite difference method to determine numerical solutions with specified boundary conditions for these equations. For a system of first-order ODEs, $\vec{x}'(t) - f(t, \vec{x}) = 0$ define

$$\vec{E}_k \equiv \vec{x}_k - \vec{x}_{k-1} - h_k f\left(\tfrac{1}{2}(t_k + t_{k-1}), \tfrac{1}{2}(\vec{x}_k + \vec{x}_{k-1})\right) = 0, \tag{10}$$

where $k = 2, 3, \ldots, M$, $h_k = t_k - t_{k-1}$ and M is the number of mesh points. If n_1 is the number of boundary conditions at the first boundary and n_2 is the number of boundary conditions at the second boundary, then $\vec{E}_1$ will have n_1 non-zero entries and $\vec{E}_{M+1}$ will have n_2 non-zero entries. Since the relaxation method is iterative, incremental changes of each dependent variable, $\Delta x_{j,k}$, between iterations must be determined. A Taylor series expansion of Eq. (10) results in

$$\vec{E}_k(\vec{x}_k + \Delta\vec{x}_k, \vec{x}_{k-1} + \Delta\vec{x}_{k-1}) \approx E_{j,k}(\vec{x}_k, \vec{x}_{k-1}) + \sum_{n=1}^{N} \frac{\partial E_{j,k}}{\partial x_{n,k-1}} \Delta x_{n,k-1} + \sum_{n=1}^{N} \frac{\partial E_{j,k}}{\partial x_{n,k}} \Delta x_{n,k}, \tag{11}$$

where $j = 1, 2, \ldots, N$, which gives $M \times N - (n_1 + n_2)$ equations representing the interior points. For the first and second boundary conditions, respectively,

$$\vec{E}_1(\vec{x}_1 + \Delta\vec{x}_1) \approx E_{j,1}(\vec{x}_1) + \sum_{n=1}^{N} \frac{\partial E_{j,1}}{\partial x_{n,1}} \Delta x_{n,1}, \tag{12}$$

$$\vec{E}_{M+1}(\vec{x}_M + \Delta\vec{x}_M) \approx E_{j,M+1}(\vec{x}_M) + \sum_{n=1}^{N} \frac{\partial E_{j,M+1}}{\partial x_{n,M}} \Delta x_{n,M}, \tag{13}$$

where $j = 1, 2, \ldots, n_1$ for Eq. (12) and $j = 1, 2, \ldots, n_2$ for Eq. (13). For the solution to converge, the left hand sides of Eqs. (11)–(13) obviously should approach zero. These equations are linear even if the differential equation is non-linear, and hence, $\Delta x_{j,k}$, can be solved for using standard methods from linear algebra such as Gaussian elimination.

Now, considering a fleet of robots operating in a coordinated manner instead of a single robot, consider a system with n robots where the desired distance between neighboring robots is specified. In that case, if we consider the cost functional

$$J = \int_0^{t_f} \left[\frac{1}{2}\sum_{i=1}^{n} u_i^2 + v_i^2 + \sum_{i=1}^{n}\left[\lambda_{x_i}\left(\dot{x}_i - \frac{r}{2}\cos\theta_i(u_i + v_i)\right)\right.\right.$$
$$\left.\left. + \lambda_{y_i}\left(\dot{y}_i - \frac{r}{2}\sin\theta_i(u_i + v_i)\right) + \lambda_{\theta_i}\left(\dot{\theta}_i - \frac{r}{2b}(u_i - v_i)\right)\right] + k\sum_{i=1}^{n-1}(d_i - \overline{d})^2\right] dt,$$

where $d_i = \sqrt{(x_i - x_{i+1})^2 + (y_i - y_{i+1})^2}$ and $\overline{d}$ is the desired distance between adjacent robots, as before.

Now, consider a system of five robots and a coordinate system where the robots are initially in a line evenly spaced between $x = 1.0$ and $x = 1.4$ along the x-axis, each with an orientation of $\theta_i = \pi/2$, and assume the final formation is where the robots are evenly distributed between $y = 1.0$ and $y = 1.4$ along the y-axis with an orientation of $\theta_i = \pi$. With the formation weighting parameter, k, set to zero, the solutions are as illustrated in Fig. 10 and because $k = 0$, the desired distance between the robots is not maintained other than at the boundaries. In the interior of the trajectories, because of the geometry of the problem, the actual distance between neighboring robots is less than the desired distance of $\overline{d} = 0.1$.

https://doi.org/10.1017/S026357471600045X Published online by Cambridge University Press

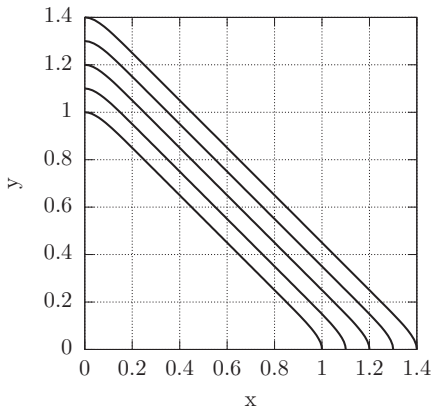


Fig. 10. Optimal solution for five-robot system when $k = 0$.

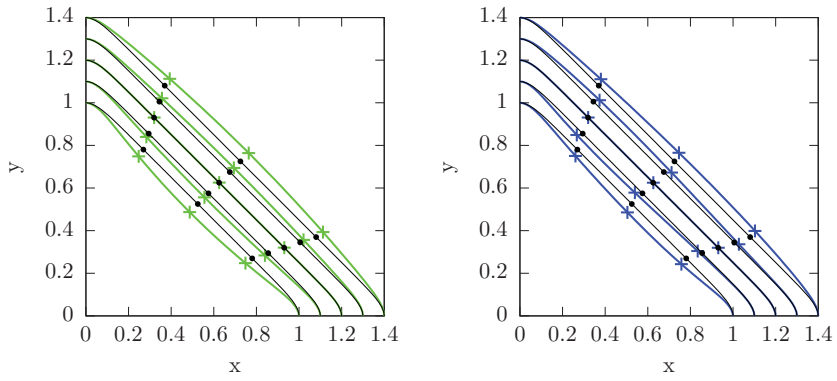


Fig. 11. Solution one (left) and two (right), positions marked at $t = 0.25$, 0.50 and 0.75 s.

If the value of the bifurcation parameter is increased to $k = 8 \times 10^5$, multiple solutions exist, five of which are illustrated in Figs. 11–13. The bifurcation parameter is large compared to the holonomic case because of the non-normalized, physically reasonable parameter values selected for the problem. The specific value of $k = 8 \times 10^5$ was selected because it was near the middle of range of values where we found five solutions, which is a large enough number to demonstrate the complexity of the problem, but small enough to clearly communicate and understand. The black dotted line in each of those figures represents the $k = 0$ solution and the green, red and blue lines are the solution for $k = 8 \times 10^5$. The crosses indicate each of the solutions at the specific points in time $t = 0.25, 0.50$ and 0.75 and the dots indicated the $k = 0$ solutions at those same points in time (recall $t \in [0, 1]$). It is clear from an analysis of the solutions in those figures that part of the nature of the multiplicity of solutions is that neighboring robots can get "ahead" or "behind" its neighbors. This allows each robot to track the $k = 0$ trajectory more closely, which minimizes the control effort, while simultaneously more closely maintaining the formation distance constraint.

Figures 11–13 illustrate multiple solutions for a fixed value of the bifurcation parameter, k. Branches of the same color in these plots correspond to the same solutions. Now, we construct bifurcation diagrams by tracking the solutions as k is varied. The relaxation method is particularly efficient for this because solutions that have already been determined may be used as the initial condition for the method. These diagrams illustrate the difference between solutions and the $k = 0$ solution for a range of k-values. Figures 14–16 are the bifurcation diagrams for this fleet of non-holonomic robots. As before, it makes sense that as k is increased the number of solutions to the boundary value problem will increase. The units for the y-axis are centimeters and the x-axis values should be times 10^5. This is because in the limit as $k \to \infty$, only maintaining the formation matters compared to the control effort. Hence, in the limit, one would expect that any trajectory which maintains distance between the robots is a solution, which is consistent with Figs. 14 through 16.

https://doi.org/10.1017/S026357471600045X Published online by Cambridge University Press

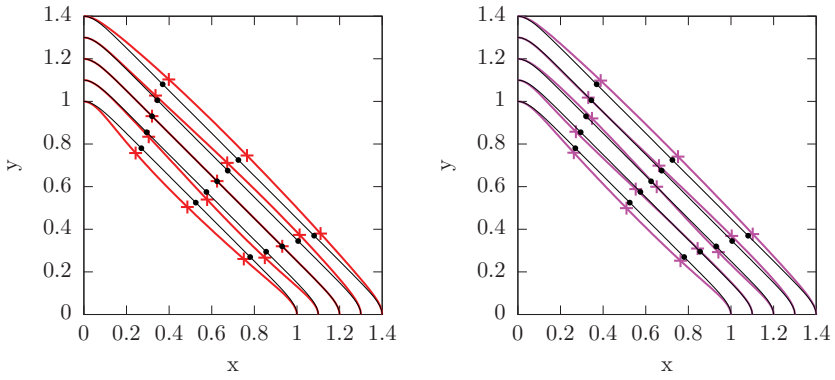


Fig. 12. Solution three (left) and four (right), positions marked at $t = 0.25$, 0.50 and 0.75 s.

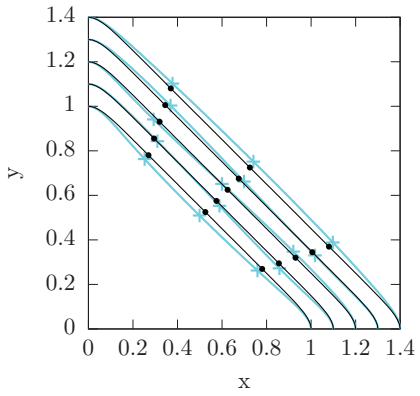


Fig. 13. Solution five, positions marked at $t = 0.25$, 0.50 and 0.75 s.

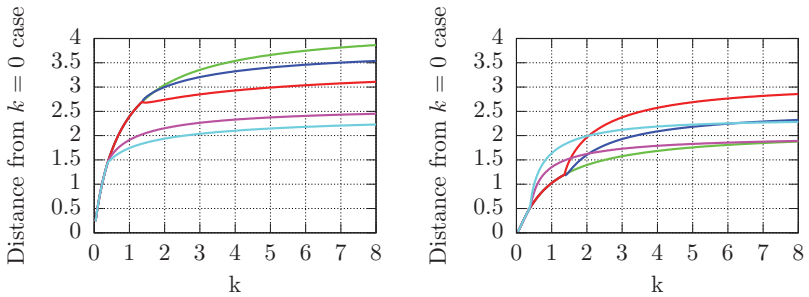


Fig. 14. Bifurcations at $t = 0.25$ for robots one (left) and two (right).

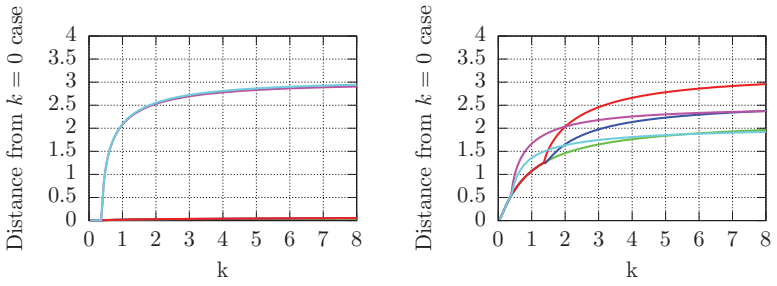


Fig. 15. Bifurcations at $t = 0.25$ for robots three (left) and four (right).

https://doi.org/10.1017/S026357471600045X Published online by Cambridge University Press

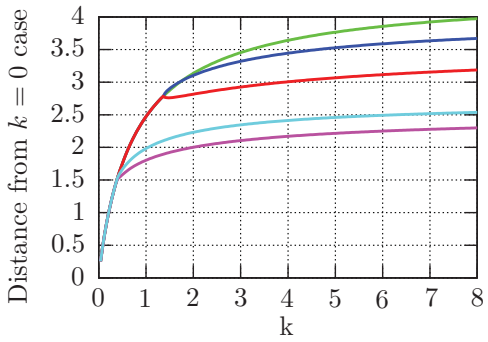


Fig. 16. Bifurcations at $t = 0.25$ for robots five.

These bifurcation results illustrate a subtle, but important distinction relative to our previous results. Specifically, for the system in Section 3 we showed that the bifurcation diagrams must be symmetric in that, for the five-robot formation problem like the one considered in this paper, the bifurcation diagrams for robots one and five must be symmetric in that they are reflections of each other, the diagrams for robots two and four must be similarly symmetric and the bifurcation diagram for robot three must be symmetric with respect to itself.

For the current system, this result does *not* hold. This is most easily seen for robots two and four at the right end (high k-values) of the bifurcation diagram where the branches cross for corresponding solutions as slightly different k-values (other differences are similarly evident). This is *not* a numerical artifact, because the persistence of this difference was investigated by a grid resolution convergence study by increasingly refining the finite difference meshes. In fact, the symmetry of the system is broken by the robot itself because the left and right wheels travel different distances along most trajectories that are not straight lines. The order of the differences between the bifurcation diagrams appears to be on the order of a couple percent, which is also approximately the order of the spacing between the wheels on the robot relative to the overall length of the trajectory. An interesting subject of current work is to determine whether the differences between the bifurcated solutions may be bounded, and if so, what sorts of computational savings may be obtained therefrom.

7. Conclusions and Future Work

This paper analyzed the nature and structure of multiple solutions to an optimal control problem for formation control for multiple mobile robots and was developed over a series of previous conference papers by some of the authors. This approach is important for robotics engineers because various forms of optimization are common in path planning algorithms in robotics and an understanding of the global structure of the solution space will lead to more efficient and optimal path planning methods and solutions.

When considering the trade-off between minimizing control effort and maintaining the desired formation, a complicated and rich solution bifurcation structure is presented. Two types of problems were considered. The first was a holonomic system in which both five and seven robot systems were considered. This holonomic system has aspects related to the dexterous manipulation problem where the robotic fingertips have spherical surfaces. The second system was the non-holonomic robot. In both cases, numerical simulation results show a unique solution when a much greater weight was given to the control effort compared to the formation cost; conversely, when the formation is given a much greater weight, many solutions are present.

In addition to the numerical investigations, there are two theoretical contributions to this paper. First, in the case of symmetric systems, we show that the bifurcation diagrams *must* be symmetric. This is useful because it is numerically expensive to search for solutions and the relationship between symmetric solutions is algebraic. Hence, when a solution is determined for a symmetric system, the second is automatically known. Second, an asymptotic analysis shows consistency with the intuitive interpretation that a greater weighting on the control effort corresponds to a unique solution and a greater weighting on the formation corresponds to multiple (many) solutions.

https://doi.org/10.1017/S026357471600045X Published online by Cambridge University Press

This investigation motivates several avenues for future research. First, a systematic means for characterizing bifurcations for boundary value problems must be developed. This seems to be an open problem without an obvious generalization for bifurcations of fixed points of dynamical systems because the entire solution, as opposed to an isolated equilibrium, is what bifurcates. This fundamentally arises because of the two-point boundary value problem nature of the optimization. Second, numerically efficient methods are necessary for searching for solutions. The shooting method and finite difference methods are only somewhat efficient for finding isolated solutions because they are iterative. Extending the methods to globally search for solutions is obviously problematic. Some initial results exist based on polynomial homotopy methods[16] but due to the manner in which the number of roots of polynomial systems grow with the order of the polynomial and dimension of the problem, such an approach does not seem to scale well. Finally, due to the utility in practical implementations, connecting these results with receding-horizon methods would be useful.

Acknowledgements

The support of the US National Science Foundation under the CPS Large Grant No. CNS-1035655 is gratefully acknowledged. The authors would also like to thank the reviewers for many helpful comments and suggestions and especially thank Professor Mihir Sen for his thoughtful and insightful conversations related to this work.

References

1. T. R. Smith, H. Hanssmann and N. E. Leonard, "Orientation Control of Multiple Underwater Vehicles with Symmetry-Breaking Potentials," *Proceedings of the IEEE Conference on Decision and Control*, Orlando, Florida, USA (2001) pp. 4598–4603.
2. C. R. McInnes, "Autonomous ring formation for a planar constellation of satellites," *AIAA J. Guid. Control Dyn.* **18**(5), 1215–1217 (1995).
3. H. Puttgen, P. MacGrego and F. Lambert, "Distributed generation: Semantic hype or dawn of a new era?" *IEEE Power Energy Mag.* **1**(1), 22–29 (2003).
4. J. Jennings, G. Whelan and W. Evans, "Cooperative Search and Rescue with a Team of Mobile Robots," *Proceedings of the IEEE International Conference on Advanced Robotics*, Monterey, California, USA (1997) pp. 193–200.
5. J. P. Desai, "Modeling Multiple Teams of Mobile Robots: A Graph Theoretic Approach," *Proceedings of the IEEE/RSJ International Conference on Intelligent Robots and Systems*, IEEE, vol. 1, Maui, Hawaii, USA (2001) pp. 381–386.
6. J. P. Desai, J. Ostrowski and V. Kumar, "Controlling Formations of Multiple Mobile Robots," *Proceedings of the IEEE International Conference on Robotics and Automation*, IEEE, vol. 4, Leuven, Belgium (1998) pp. 2864–2869.
7. N. E. Leonard and E. Fiorelli, "Virtual Leaders, Artificial Potentials, and Coordinated Control of Groups," *Proceedings of the IEEE Conference on Decision and Control*, Orlando, Florida, USA (2001) pp. 2968–2973.
8. T. Balch and R. Arkin, "Behavior-based formation control for multi-robotic teams," *IEEE Trans. Robot. Autom.* **14**(6), 926–934 (1998).
9. T. Balch and M. Hybinette, "Behavior-Based Coordination of Large-Scale Robot Formations," *Proceedings of the 4th International Conference on MultiAgent Systems*, IEEE (2000) pp. 363–364.
10. Z. Su and J. Lu, "Formation feedback applied to behavior-based approach to formation keeping," *J. Beijing Inst. Technol.* **13**(2), 190–193 (2004).
11. C. Belta and V. Kumar, "Geometric Methods for Multirobot Optimal Motion Planning," **In**: *Handbook of Geometric Computing* (E. B. Corrochano, ed.) (Springer, 2005) pp. 679–706.
12. M. A. Lewis and K. H. Tan, "High precision formation control of mobile robots using virtual structures," *Auton. Robots* **4**(4), 387–403 (1997).
13. K.-H. Tan and M. A. Lewis, "Virtual Structures for High-Precision Cooperative Mobile Robotic Control," *Proceedings of the IEEE/RSJ International Conference on Intelligent Robots and Systems*, Osaka, Japan (1996) pp. 132–139.
14. R. M. Murray, "Recent research in cooperative control of multivehivle systems," *J. Dyn. Syst. Meas. Control* **129**(5), 571–583 (2007).
15. B. Deng, M. Sen and B. Goodwine, "Bifurcations and Symmetries of Optimal Solutions for Distributed Robotic Systems," *Proceedings of the American Control Conference*, Saint Louis, Missouri, USA (2009) pp. 4127–4133.
16. B. Deng, A. K. Valenzuela. and B. Goodwine, "Bifurcations of Optimal Solutions For Coordinated Robotic Systems: Numerical and Homotopy Methods," *Proceedings of the IEEE International Conference on Robotics and Automation*, Anchorage, Alaska, USA (2010) pp. 4475–4480.

https://doi.org/10.1017/S026357471600045X Published online by Cambridge University Press

17. M. O'Connor and B. Goodwine, "Symmetry-Breaking in Bifurcations of Optimal Solutions for Coordinated Nonholonomic Robotic Control," *Proceedings of the 20th Mediterranean Conference on Control and Automation*, Barcelona, Spain (2012) pp. 1554–1559.
18. B. Goodwine, "Towards Some General Results in Bifurcations In Optimal Solutions For Symmetric Distributed Robotic Formation Control," *Proceedings of the IEEE/SICE International Symposium on System Integration (SII)*, Nagoya, Japan (2015) pp. 358–363.
19. L. H. Erbe and H. Wang, "On the Existence of Positive Solutions of Ordinary Differential Equations," *Proc. Amer. Math. Soc.* **120**(3), 743–748 (1994).
20. L. Erbe, S. Hu and H. Wang, "Multiple positive solutions of some boundary value problems," *Math. Anal. Appl.* **184**, 743–748 (1994).
21. Y. Naito and S. Tanaka, "On the existence of multiple solutions of the boundary value problem for nonlinear second-order differential equations," *Nonlinear Anal.* **56**(4), 919–935 (2004).
22. R. Ma and B. Thompson, "Multiplicity results for second-order two-point boundary value problems with nonlinearities across several eigenvalues," *Appl. Math. Lett.* **18**(5), 587–595 (2005).
23. J. Marcos do Ó, S. Lorca and P. Ubilla, "Local superlinearity for elliptic systems involving parameters," *J. Differ. Equ.* **211**(1), 1–19 (2005).
24. R. I. Avery and J. Henderson, "Three symmetric positive solutions for a second-order boundary value problem," *Appl. Math. Lett.* **13**(3), 1–7 (2000).
25. H. Amann and J. López-Gómez, "A priori bounds and multiple solutions for superlinear indefinite elliptic problems," *J. Differ. Equ.* **146**(2), 336–374 (1998).
26. G. L. Karakostas and P. Ch Tsamatos, "Existence of multiple positive solutions for a nonlocal boundary value problem," *J. Juliusz Schauder Center* **19**, 109–121 (2002).
27. D. S. Cohen, "Multiple stable solutions of nonlinear boundary value problems arising in chemical reactor theory," *SIAM J. Appl. Math.* **20**(1), 1–13 (1971).
28. P. J. Y. Wong and R. P. Agarwal, "Multiple positive solutions of two-point right focal boundary value problems," *Math. Comput. Modelling* **28**(3), 41–49 (1998).
29. Z. Yang, "Existence and uniqueness of positive solutions for an integral boundary value problem," *Nonlinear Anal.: Theory Methods Appl.* **69**(11), 3910–3918 (2008).
30. J. Mawhin and M. Willem, "Multiple solutions of the periodic boundary value problem for some forced pendulum-type equations," *J. Differ. Equ.* **52**(2), 264–287 (1984).
31. A. Cabada, A. Iannizzotto and S. Tersian, "Multiple solutions for discrete boundary value problems," *J. Math. Anal. Appl.* **356**(2), 418–428 (2009).
32. R. P. Agarwal, K. Perera and D. O'Regan, "Multiple positive solutions of singular and nonsingular discrete problems via variational methods," *Nonlinear Anal.: Theory Methods Appl.* **58**(1), 69–73 (2004).
33. X. Lin and D. Jiang, "Multiple positive solutions of dirichlet boundary value problems for second order impulsive differential equations," *J. Math. Anal. Appl.* **321**(2), 501–514 (2006).
34. H. Wang, "On the number of positive solutions of nonlinear systems," *J. Math. Anal. Appl.* **281**(1), 287–306 (2003).
35. K. Q. Lan, "Multiple positive solutions of semilinear differential equations with singularities," *J. London Math. Soc.* **63**(3), 690–704 (2001).
36. R. I. Avery and D. R. Anderson, "Existence of three positive solutions to a second-order boundary value problem on a measure chain," *J. Comput. Appl. Math.* **141**(1), 65–73 (2002).
37. J. Henderson and H. B. Thompson, "Existence of multiple solutions for second order boundary value problems," *J. Differ. Equ.* **166**(2), 443–454 (2000).
38. D. Anderson, "Multiple positive solutions for a three-point boundary value problem," *Math. Comput. Modelling* **27**(6), 49–57 (1998).
39. W.-C. Lian, F.-H. Wong and C.-C. Yeh, "On the existence of positive solutions of nonlinear second order differential equations," *Proceedings of the American Mathematical Society* **124**(4), 1117–1126 (1996).
40. Z. Liu and F. Li, "Multiple positive solutions of nonlinear two-point boundary value problems," *J. Math. Anal. Appl.* **203**(3), 610–625 (1996).
41. R. M. Murray, Z. Li and S. S. Sastry, *A Mathematical Introduction to Robotic Manipulation* (CRC Press, Inc., Boca Raton, Ann Arbor, London and Tokyo, 1994).
42. B. Siciliano and O. Khatib, eds. *Springer Handbook of Robotics* (Springer-Verlag, Berlin, Heidelberg, 2008). Chapter 41.
43. J. Stoer and R. Bulirsch, *Introduction to Numerical Analysis* (Springer-Verlag, New York, 1980).
44. W. H. Press, S. A. Teukolsky, W. T. Vetterling and B. P. Flannery, *Numerical Recipes: The Art of Scientific Computing*, 3rd ed. (Cambridge University Press, Cambridge, New York, Melbourne, 2007).
45. J. Kevorkian, *Perturbation Methods in Applied Mathematics* (Springer-Verlag, New York, 1981).
46. H. K. Khalil, *Nonlinear Systems* (Macmillan Publishing Company, New York, 1992).
47. B. Deng, Bifurcations and Symmetries of Optimal Solutions for Distributed Robotic Systems *Ph.D. Thesis* (University of Notre Dame, New York, 2011).
48. M. Brett McMickell and B. Goodwine, "Motion planning for nonlinear symmetric distributed robotic formations," *Int. J. Robot. Res.* **27**(10), 1025–1041 (2007).
49. M. Brett McMickell and B. Goodwine, "Reduction and controllability of nonlinear symmetric distributed systems," *Int. J. Control* **76**(18), 1809–1822 (2003).

https://doi.org/10.1017/S026357471600045X Published online by Cambridge University Press

50. B. Goodwine, "Compositional Boundedness of Solutions for Symmetric Nonautonomous Control Systems," *Proceedings of the Mediterranean Conference on Control and Automation (MED)*, Palermo, Italy (2014) pp. 798–803.
51. A. Nettleman and B. Goodwine, "Symmetries of Multiagent Systems and Formation Stability," *Proceedings of the International Symposium on Mathematical Theory of Networks and Systems (MTNS)*, Groningen, The Netherlands (2014) pp. 1340–1343. Extended abstract review.
52. B. Goodwine, "Nonlinear Stability of Approximately Symmetric Large-Scale Systems," *Proceedings of the International Federation of Automatic Control World Congress (IFAC)*, Cape Town, South Africa (2014) pp. 845–850.
53. A. Nettleman and B. Goodwine, "Symmetries and Reduction for Multi-Agent Control," *Proceedings of the IEEE International Conference on Robotics & Automation (ICRA)*, Seattle, Washington, USA (2015) pp. 5390–5396.
54. B. Goodwine and P. Antsaklis, "Multi-agent compositional stability exploiting system symmetries," *Automatica* **49**(11), 3158–3166 (2013).
55. M. Brett McMickell, B. Goodwine and L. Antonio Montestruque, "Micabot: A Robotic Platform for Large-Scale Distributed Robotics," *Proceedings of the IEEE International Conference on Robotics and Automation*, Taipei, Taiwan (2003) pp. 1600–1605.

https://doi.org/10.1017/S026357471600045X Published online by Cambridge University Press